ACS Symp. Ser. 353, 176-199 (1987)

Chapter 11

Sensitivity of Vibrational and Rotational Energy Transfer to the Potential Energy Surface in the Collision of Two Molecules

Large-Scale Quantum Mechanical Calculations

David W. Schwenke and Donald G. Truhlar

Minnesota Supercomputer Institute and Department of Chemistry, University of Minnesota, Minneapolis, MN 55455

We present an overview of our research program on HF-HF collisions, including potential energy surfaces and dynamics calculations, with special emphasis on the sensitivity of the dynamics results to the choice of surface.

The molecules of a gas in a thermally equilibrated state are characterized by a Boltzmann distribution of vibrational and rotational states. Although energy is transferred between modes in individual collisions, there is no net change in the vibrational-rotational distributions. If the equilibrium populations are perturbed in any way, e.g., by heating, cooling, the influx of laser light, or a chemical reaction, then the system will relax to a new equilibrium distribution (1). The change of vibrational state populations with time is usually much slower than the rotational relaxation, but it is critical for understanding many classes of nonequilibrium processes. For example if an exothermic chemical reaction like

$$F + H_2 \rightarrow HF + H$$

or

$$H + F_2 \rightarrow HF + F$$

produces vibrationally excited products — HF in the examples — the competition between vibrational-rotational-state redistribution and stimulated emission is critical in determining whether energy can be extracted in the form of infrared laser action. Another example concerns the attempt to force reactions to yield nonspontaneous products by using laser light to pump a selected vibrational mode of a polyatomic molecule, e.g., the stretching vibration of a bond that it is desired to break. If the energy is redistributed rapidly compared to the time scale for the reaction, only the usual products of the reaction that occurs spontaneously upon slow heating will be observed.

0097-6156/87/0353-0176$07.00/0

The simplest models of energy transfer involve an atom and a nonrotating oscillator or an atom and a rigid rotator. But the single oscillator model is insufficient for molecule-molecule collisions or even atomic collisions with a polyatomic molecule because processes involving the transfer of energy between vibrational modes, called vibrational-to-vibrational (V-V) or vibrational-to-vibrational-and-rotational (V-V,R) energy transfer, are usually much more efficient than those involving vibrational-to-translational (V-T) or vibrational-to-translational-and-rotational (V-T,R) energy transfer (2). Furthermore, the coupling of rotational and vibrational degrees of freedom can change the quantitative values of the transition probabilities for vibrational state changes by an order of magnitude or more.

One of the goals of modern scattering theory is the rigorous solution of the quantum mechanical equations governing molecular collisions. Prior to supercomputers, one could solve the equations for the atom-oscillator and atom-rigid-rotator models or for light enough atom-diatom systems at low energy (3). But in order to treat V-V and V-V,R processes accurately, we must do calculations on systems with two or more vibrational degrees of freedom, coupled to rotations, at energies above the second vibrational threshold (the energetic requirement arises because different excited vibrational states are populated before and after the collision for a V-V or V-V,R process). The problem with doing this is one of computational economy. As either the number of degrees of freedom or the energy is increased, the number N of basis functions required to expand the scattering wave function increases dramatically. For conventional methods of solving the quantum mechanical equations, though, the computer time scales as N^3 and the memory required, which can also be significant, scales as N^2. Thus one rapidly reaches a point where the calculation becomes impossible on any machine — past, present, or presently envisaged. Nevertheless, with supercomputers one can push the boundaries of feasibility into a new realm, and we have embarked on a study designed to do so. In particular we have made large-scale calculations for the process

$$HF(v_1=1,j_1=0) + HF(v_2=1,j_2=0) \rightarrow HF(v_1'=2,j_1') + HF(v_2'=0,j_2') \qquad (1)$$

where the (unprimed, primed) $v_i(i=1,2)$ are (initial, final) vibrational quantum numbers, and j_1, j_2, j_1', j_2' are rotational quantum numbers with the same conventions.

Since HF has a closed-shell electronic structure and no low-lying excited electronic states, HF-HF collisions may be treated quite adequately within the framework of the Born-Oppenheimer electronic adiabatic approximation. In this treatment (4) the electronic and coulombic energies for fixed nuclei provide a potential energy V for internuclear motion, and the collision dynamics is equivalent to a four-body problem. After removal of the center-of-mass coordinates, the Schroedinger equation becomes nine-dimensional. This nine-dimensional partial differential

D. W. Schwenke and D. G. Truhlar, in *Supercomputer Research in Chemistry and Chemical Engineering*, edited by K. F. Jensen and D. G. Truhlar (American Chemical Society Symposium Series Volume 353, Washington, 1987), pp. 176-199.

equation is then converted to N coupled ordinary differential equations by expanding the solution in symmetrized internal-state eigenfunctions (5-7) (which is called the close coupling approximation and is described further below). These coupled differential equations must be solved subject to scattering boundary conditions, and this is accomplished by an invariant-embedding-type (8-10) propagation method (11,12) involving repeated operations on matrices of order N.

Although our work is primarily directed to the second — dynamical — step, it is necessary for us to start with the potential energy function V. Unfortunately, as is often the case for systems whose dynamics we wish to study, a completely satisfactory V function for HF-HF collisions is unavailable. Thus we constructed two new approximate V functions (13-16) and we considered five potential functions developed by others (17-21) and we performed large-scale (N > 250) calculations (13-16,22-24) for several (13-17,19,21) of these. In some calculations we treated the vibrations as rigid and considered only translational-to-rotational (T-R) energy transfer. This reduces the number of degrees of freedom from 9 to 7 and hence reduces computational complexity, but it provides a valuable test of the dynamical significance of the differences in the various V functions because the final rotational state distributions of the rigid-rotator calculations are primarily sensitive to the anisotropy of V. We have also performed large-scale calculations including the vibrational coordinates for three of the V functions. In one case the transition probabilities for process (1) are well converged; unfortunately the potential for that case may be inaccurate. Nevertheless converged quantal dynamics calculations for any given V provide a benchmark for testing approximate quantal, semiclassical, and classical methods of collision dynamics, and the present results also demonstrate the feasibility — for an expenditure of more computational resources — of obtaining converged quantal dynamics solutions for more realistic V functions.

The above constitutes a general overview of our quantum mechanical calculations so far (13-16,22-24) on process (1) and rigid-rotator HF-HF collisions. In the sections below we provide further details of selected subtopics in this research program. Section 2 reviews the potential functions we have studied; section 3, the dynamics method; section 4, the results for rigid-rotator collisions; and section 5, the results for process (1). Throughout this overview we place special emphasis on the comparison of the various surfaces and of the dynamical results obtained with one surface to those obtained with another. Another long-range goal of our program, though, is to use converged quantal studies of the dynamics as benchmarks for testing more approximate theories; in this regard, it should be *especially* interesting to test semiclassical (25-27) and quasiclassical (28-31) theories of V-V, R energy transfer.

Potential Energy Surfaces

The rigid-rotator collisions may be taken as a model for

$$HF(v_1=0,j_1) + HF(v_2=0,j_2) \rightarrow HF(v_1'=0,j_1') + HF(v_2'=0,j_2') \quad (2)$$

We have carried out converged rigid-rotator dynamics calculations for four potentials:

Abbreviation	Reference
AD	Alexander and DePristo (17)
BM	Brobjer and Murrell (19)
RB	Redmon and Binkley (21)
RBST	Reference 16

These surfaces are all based on some combination of *ab initio* electronic structure calculations plus fitting. The AD and BM surfaces are based respectively in whole or in part on extended-basis-set single-configuration self-consistent-field calculations, whereas the RB and RBST calculations are based on calculations including electron correlation by Moller-Plesset fourth-order perturbation theory. For the rigid-rotator calculations R_1 the intramolecular internuclear distances R_1 and R_2 are fixed at 1.733 a_0. The rigid-rotator interaction potential may be expanded as

$$V_{int} = \sum_{q_1 q_2 \mu} v_{q_1 q_2 \mu}(r)\, {}^{q}y_{q_1 q_2 \mu}(\hat{r}_1, \hat{r}_2) \quad (3)$$

where

$${}^{q}y_{q_1 q_2 \mu} = \frac{4\pi}{[2(1+\delta_{\mu 0})]^{1/2}} [Y_{q_1 \mu}(\hat{r}_1) Y_{q_2 -\mu}(\hat{r}_2) + Y_{q_1 -\mu}(\hat{r}_1) Y_{q_2 \mu}(\hat{r}_2)] \quad (4)$$

$Y_{q_i \mu}$ is a spherical harmonic, r is the distance between the molecular centers of mass, and $\hat{r}_1$ and $\hat{r}_2$ are unit vectors along the molecular axes in a ("body-fixed") frame of reference in which the z axis is along the vector connecting the molecular centers of mass. The first several nonzero coefficients are compared for the four surfaces in Figures 1-6. We see qualitatively good agreement for the general shape of the r dependence in all cases, but apparently significant quantitative differences. To get a better understanding of the effect of these quantitative differences, we consider the transition probabilities calculated with the various surfaces for processes (2) in Section 4.

The AD and BM surfaces are based on *ab initio* calculations carried out only for $R_1 = R_2 = R_e$, where R_e is the value for an isolated diatom. Thus the AD and BM surfaces cannot be used to study V-V and V-V,R (or V-T) energy transfer.

To study processes involving vibration we must add the two diatomic vibrational potentials to V_{int} and we must also generalize V_{int} to include a dependence on vibrational coordinates. The AD surface was extended to include all geometries by adding two kinds

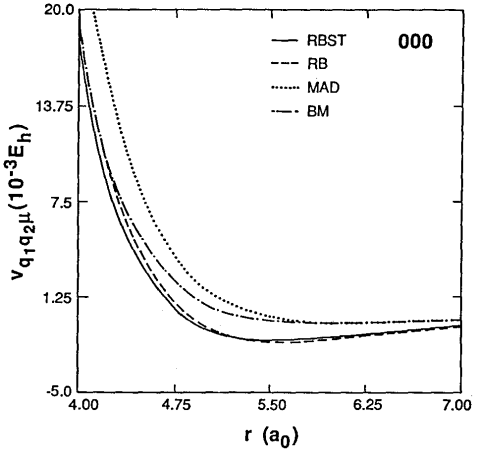

Figure 1. Body-frame expansion coefficients (in hartrees) of eq. (3) for rigid-rotator HF-HF collisions as functions of the collisional separation coordinate r (in bohrs) for $q_1 = q_2 = \mu = 0$.

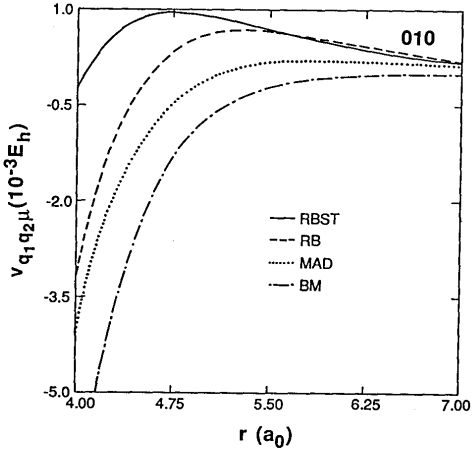

Figure 2. Same as Fig. 1 except $q_1 = \mu = 0$, $q_2 = 1$.

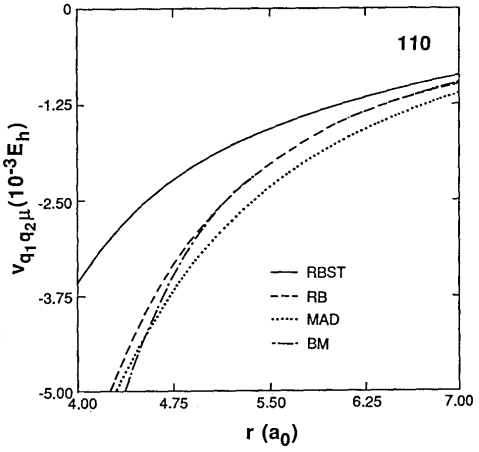

Figure 3. Same as Fig. 1 except $q_1 = q_2 = 1$, $\mu = 0$.

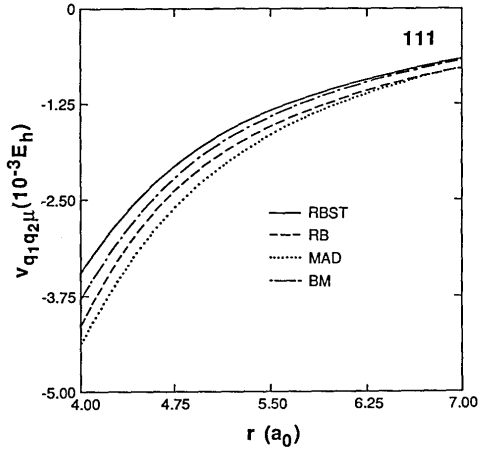

Figure 4. Same as Fig. 1 except $q_1 = q_2 = \mu = 1$.

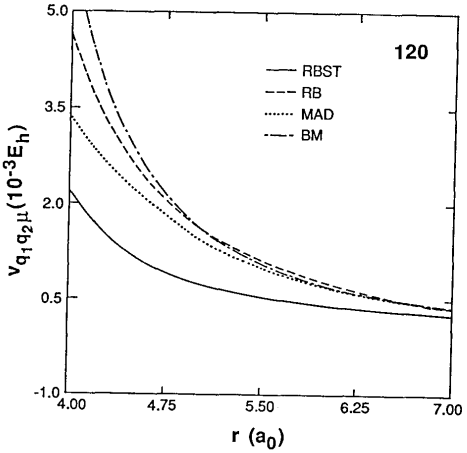

Figure 5. Same as Fig. 1 except $q_1 = 1$, $q_2 = 2$, $\mu = 0$.

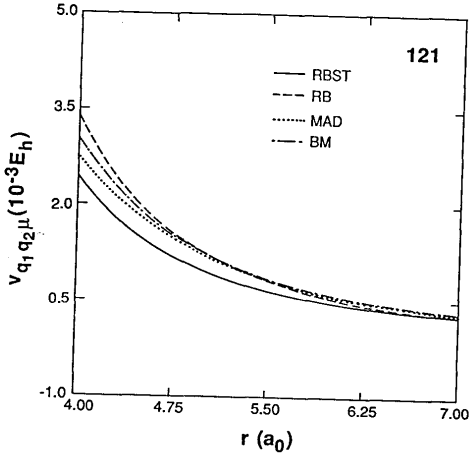

Figure 6. Same as Fig. 1 except $q_1 = \mu = 1$, $q_2 = 2$.

of dependence on the intramolecular H-F distances R_1 and R_2. The long-range (large r) dependence on R_1 and R_2 was based on the known dependence (32,33) of the permanent dipole and quadrupole moments on internuclear distance. This may be reasonable since HF-HF interactions are dominated by electrostatic terms at and beyond the van der Waals hydrogen-bonded minimum (34). The dependence of the potential on R_1 and R_2 at short range (small r) was included by an approximation based on the idea that when a single interatomic potential dominates the short-range repulsion, the gradient of the whole potential is a function of only the pair distance and so there is a simple geometrical relation between the gradient with respect to changing this distance by changing r and the gradients with respect to changing this distance by changing R_1 and R_2.

These simple relations motivate a more formal approximation in which we first re-expand the interaction potential in a space-fixed ("laboratory-frame") coordinate system as

$$V_{int} = (4\pi)^{3/2} \sum_{\lambda_1\lambda_2\lambda} U_{\lambda_1\lambda_2\lambda}(r) Y_{\lambda_1\lambda_2\lambda}(\hat{r},\hat{R}_1,\hat{R}_2) \qquad (5)$$

where

$$Y_{\lambda_1\lambda_2\lambda} = \sum_{m_1m_2m} (\lambda_1 m_1 \lambda_2 m_2 | \lambda_1\lambda_2\lambda m) Y_{\lambda_1 m_1}(\hat{R}_1) Y_{\lambda_2 m_2}(\hat{R}_2) Y^*_{\lambda m}(\hat{r}) \qquad (6)$$

$(\cdots|\cdots)$ is a Clebsch-Gordan coefficient, and the $\hat{R}_i$ are unit vectors along the bond axes in the space-fixed system, and then we make the $U_{\lambda_1\lambda_2\lambda}$ depend exponentially on R_1 and R_2 with exponential range parameters based on the r dependence of the potential (13-15). This kind of parameterization was first applied to a breathing-sphere model of HF-HF by Gianturco *et al.* (35). The resulting potential in the present case is called the MAD potential, which denotes "modified AD".

The Redmon-Binkley potential is a multi-center fit of *ab initio* calculations including *separate* variations of R_1 and R_2. The fit was based on minimizing the root-mean-square (rms) value of the difference between the fit values and the originally calculated potential values. The RBST potential differs in three ways: (i) The *ab initio* data set was augmented by over 100 points in which R_1 and R_2 were *simultaneously* different from R_e. (ii) The surface was refit by making local fits to the separate vibrational forces, $-\partial V/\partial R_1$ and $-\partial V/\partial R_2$, the cross correlation of the forces, $\partial^2 V/\partial R_1 \partial R_2$, and both principal second derivatives, $\partial^2 V/\partial R_1^2$, and $\partial^2 V/\partial R_2^2$, and then minimizing the relative rms errors in the global fits to the local forces and cross correlation of forces as well as to the potential itself. (iii) For convenience, the new fit was

made directly in terms of the body-frame expansion (3) with a restriction to only 23 terms in the sum. Because of the restriction on the sum, this surface may represent the higher-order angular anisotropy less accurately than the RB potential, especially at high energies, but because of difference (ii) it should be more accurate for the vibrational forces and cross correlation of the forces that would be expected (36) to be very important for V-V and V-V,R energy transfer. Both the RB and RBST surfaces, however, are believed to yield more accurate vibrational forces and vibrational force cross correlations than the MAD surface because they are based on highly correlated *ab initio* calculations at over 1300 geometries (over 1400 for the RBST surface). These *ab initio* calculations (16,21) required over 70 hours of computer time on Cray-1 computers, and they would not have been possible without supercomputer resources. Thus, in summary, we performed large-scale dynamics calculations for three potential energy surfaces for the vibrating rotator case:

Abbreviation	Reference
MAD (modified AD)	References 13-15
RB	Redmon-Binkley (21)
RBST	Reference 16

Figures 7-11 show potential energy contours for two-dimensional cuts through these three surfaces. The contour sets are labelled by θ_1, θ_2, and ϕ where the z axis points from molecule 1 to molecule 2, θ_i and ϕ_i are the colatitude and longitude of the vector from F to H in molecule i ($\theta_i = 0$ if this vector points along +z), and $\phi = \phi_1 - \phi_2$. Figures 7 and 8 are for the collinear geometries FH...FH and HF...HF, respectively, Figures 9 and 10 are for planar F...FH and FH...F geometries, and Figure 11 is for a nonplanar geometry. In all cases R_2 refers to the molecule on the right. Notice that for all geometries the vibrational force on the repulsive wall is positive for the MAD potential but negative for the RB and RBST potentials. For the collinear geometries the negative force appears more physical since stretching one of the molecules increases the strongest pair repulsion. For the other geometries the determination of the correct force is more problematic.

Much additional work on HF-HF potentials, as discussed elsewhere (37,38), is directed very specifically at that part of the potential energy surface that governs the binding energy, geometry, and internal dynamics of the $(HF)_2$ dimer near its equilibrium geometry. Since a knowledge of only this limited part of the potential energy surface is insufficient to study the collision dynamics, we do not further review these studies here.

Close Coupling Formalism

The close coupling formalism employed for the present calculations

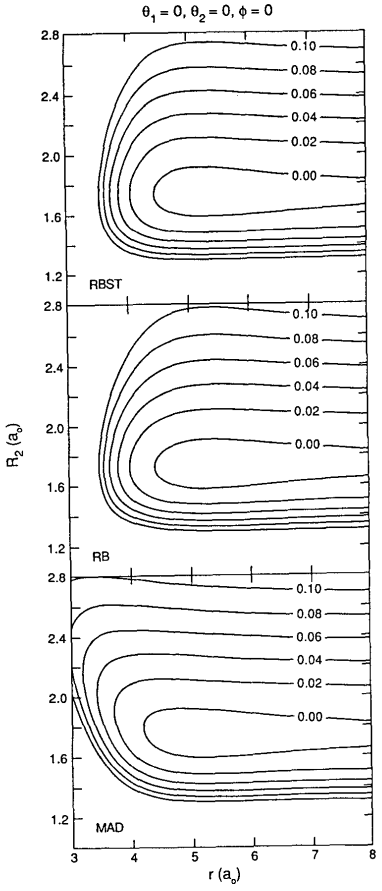

Figure 7. Two-dimensional cuts through the potential energy surface for planar HF-HF collisions including vibration. The quantity plotted in the figure is the total potential (in hartrees), which is defined as the sum of the interaction potential and the two diatomic potentials, with the zero of energy corresponding to two infinitely separated HF molecules, each at its classical equilibrium separation. This figure shows cuts through the r, R_2 plane (in bohrs) for $\theta_1 = \theta_2 = \phi = 0$ and $R_1 = 1.733\ a_0$.

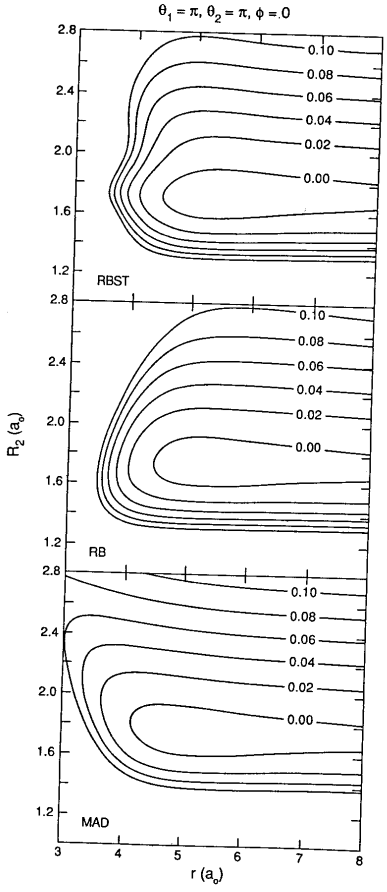

Figure 8. Same as Fig. 7 except for $\theta_1 = \theta_2 = 180^\circ$.

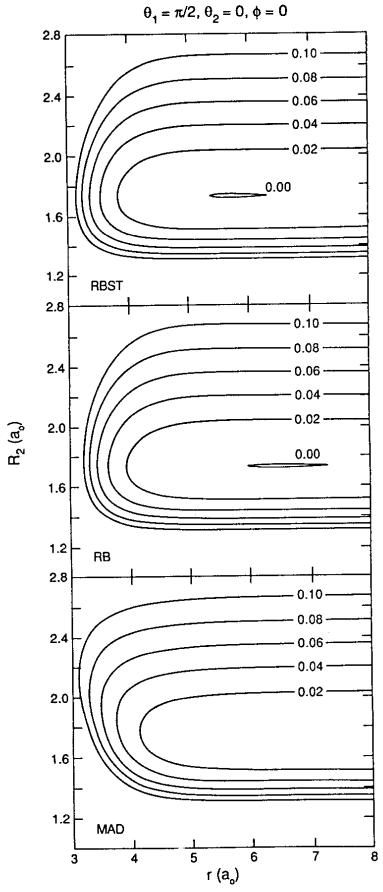

Figure 9. Same as Fig. 7 except for $\theta_1 = 90^\circ$, $\theta_2 = 0$.

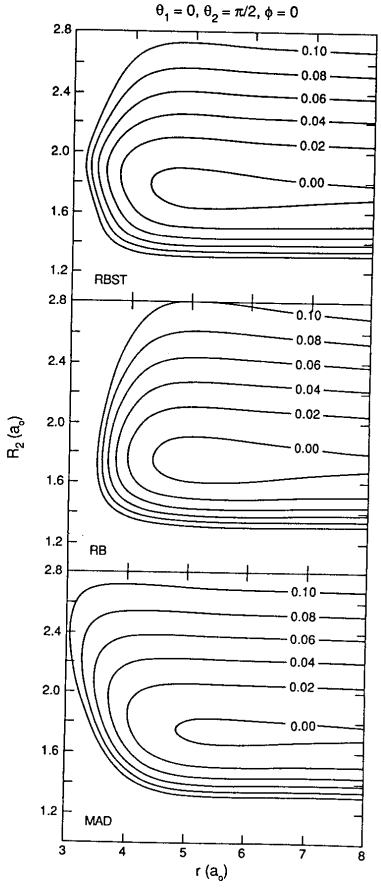

Figure 10. Same as Fig. 7 except for $\theta_1 = 0$, $\theta_2 = 90^\circ$.

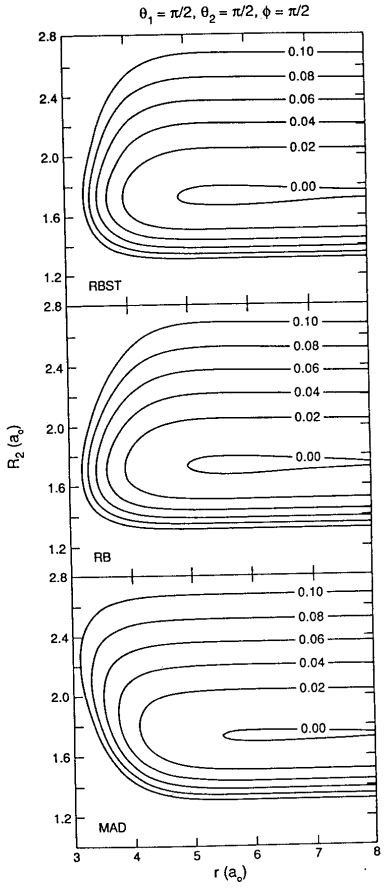

Figure 11. Same as Fig. 7 except for $\theta_1 = \theta_2 = \phi = 90^\circ$.

is described in detail elsewhere (6,7,22). In summary it involves expanding the scattering wave function in a set of symmetrized basis functions that are simultaneous eigenfunctions of the sum of the diatomic Hamiltonians (with eigenvalues ϵ_n), of the angular momentum operators j_{12}^2 (square of the vector sum of the diatomic rotational angular momenta), ℓ^2 [square of the orbital angular momentum of relative motion of the two molecules, with eigenvalues $\ell_n(\ell_n+1)\hbar^2$)], J^2 (square of the total angular momentum), and M_J (the component of the total angular momentum along a space-fixed axis), and of the parity and molecular interchange operators. Denoting these symmetrized eigenfunctions by X_n we write

$$\psi^{n_o}(\vec{r},\vec{R}_1,\vec{R}_2,E) = \frac{1}{r}\sum_{n=1}^{N} f_{nn_o}(r,E)X_n(\vec{R}_1,\vec{R}_2,\hat{r}) \qquad (7)$$

where r and $\hat{r}$ are the radial and angular parts of the intermolecular vector $\vec{r}$; and $\vec{R}_1$ and $\vec{R}_2$ are the molecular internuclear vectors; n_o denotes the intial channel (set of quantum numbers); n denotes a general channel; f_{nn_o} is the radial wave function for relative translational motion; and E is the total energy. Substituting (1) into the time-independent Schroedinger equation yields

$$\frac{d^2}{dr^2}\underset{\sim}{f}(r,E) = \underset{\sim}{D}(r,E)\underset{\sim}{f}(r,E) \qquad (8)$$

where

$$D_{nm}(r,E) = \frac{2\mu}{\hbar^2}V_{nm}(r) + \delta_{nm}\left[\frac{\ell_n(\ell_n+1)}{r^2} + \frac{2\mu(\epsilon_n-E)}{\hbar^2}\right] \qquad (9)$$

and

$$V_{nm}(r) = \int d\vec{R}_1 d\vec{R}_2 d\hat{r} X_n^*(\vec{R}_1,\vec{R}_2,\hat{r})V_{int}(\vec{R}_1,\vec{R}_2,\vec{r})X_m(\vec{R}_1,\vec{R}_2,\hat{r}) \qquad (10)$$

The integrals (10) are calculated by evaluating the expansion coefficients of Equation (3) by

$$v_{q_1q_2\mu}(r,R_1,R_2) = \frac{1}{4\pi}\int_{-1}^{1}\frac{d\cos\phi}{\sin\phi}\int_{-1}^{1}d\cos\theta_1\int_{-1}^{1}d\cos\theta_2 y_{q_1q_2\mu}V_{int}(\vec{r},\vec{R}_1,\vec{R}_2) \qquad (11)$$

The integrals in (11) are evaluated by Gaussian quadrature for each

value of r for the rigid rotator calculations and for each combination of r, R_1, and R_2 for the vibrating rotator calculations. The sum in the expansion (3) is truncated at M terms, and the calculations should be converged with respect to increasing M. Having obtained this expansion the angular integrals of (10) are performed analytically. For the vibrating rotator calculations this still leaves two integrals over vibrational coordinates and these are performed numerically by an "optimal" quadrature (39), typically with 7 points per degree of freedom.

We solve Equation (8) by an invariant imbedding (8-10) procedure, in particuilar by the R matrix propagation (11,12) method. In this method we partition the significant range of r into about 300 sectors, we propagate the solution matrix across each sector in turn, and we match solutions at sector boundaries to construct a global solution. To make the propagation step analytic in each sector, we diagonalize $\underset{\sim}{D}$ at each sector boundary. To avoid repeating the diagonalization step for each E for which a solution is sought, we propagate the solutions for several (typically 3-7) energies simultaneously. Then we need to calculate V and diagonalize D only once for a variable-energy sequence of calculations with a given J on a given potential energy surface.

Since the calculation of V scales as N^2M but the work involved in diagonalizing D and propagating the solution of (8) scales as N^3, the V calculation should become a negligible part of the calculation for large N. However, even for N > 500, if the number of terms in the expansion (3) of the potential is large, the V calculation may involve considerable CPU time, e.g., one to several hours on a supercomputer. The N^3 steps take up to 17 hours of supercomputer time for the largest single run (a 3-energy run with N = 948) involved in the present study. All calculations are vectorized, and production runs were carried out on Cray-1 and Cyber 205 computers.

Rigid Rotator Calculations (14,16,23,24)

In the present overview we concentrate our attention on calculations with $J=j_1=j_2=j_{12}=\ell=0$. J is a conserved quantity and the final values of the other quantum numbers are denoted j_1', j_2', j_{12}', and ℓ'. We will also use the notation

$$j'_{sum} = j_1' + j_2' \qquad (12)$$

(Do not confuse this simple sum with the magnitude j_{12}' of the vector sum.) Because the molecules are identical the final energy states are labelled by an un-ordered pair of rotational quantum numbers j_1' and j_2' (40). Since the order is not significant we use the convention $j_1' \leq j_2'$. For given values of J, j_1', and j_2', the quantum numbers ℓ' or j_{12}' may take on all values allowed by the triangle relations. Since J = 0 though, $j_{12}' = \ell'$. Summing the

transition probabilities over j'_{12} (or equivalently over ℓ') yields values called $P^R_{j'_1 j'_2}$, and summing these over all pairs of $j'_1 \leq j'_2$ consistent with a given value of j'_{sum} yields values called $P^R_{j'_{sum}}$.

The AD and RBST potentials are *defined* in terms of Equation (3) and have finite M values of 9 and 23, respectively. The BM and RB potentials must be re-expressed as in (3) — by using Equation (11) — and in these cases we converged the dynamics results with respect to increasing M, yielding the (unexpectedly large) values of 525 and 825, respectively. The calculations must also be converged with respect to increasing the number of channels N. We did this, and the final calculations involve N = 285 for the AD potential and N = 440 for the other potentials.

Table 1 compares $P^R_{j'_{sum}}$ values for all four potentials at a relative translational energy, E_{rel}, of 76 meV. We see a great qualitative difference between the results for the AD potential and the others, with smaller differences between the BM, RB, and RBST potentials. Evidently the restriction M = 9 is a serious limitation, greatly decreasing the rotational inelasticity, but the simplifications of the angular anisotropy in the M = 23 potential are less serious.

Table 1. Rigid-rotator transition probabilities for four potentials for E_{rel} = 76 meV

j'_{sum}	AD	BM	RB	RBST
0	0.934	0.248	0.031	0.211
1	0.004	0.025	0.077	0.055
2	0.047	0.152	0.120	0.074
3		0.105	0.030	0.082
4		0.228	0.228	0.151
5		0.051	0.119	0.141
6		0.191	0.394	0.286

Under some circumstances the rotationally anisotropy may be even further simplified for T-R energy transfer of polar molecules like HF (41). To explore this quantitatively we performed additional rigid-rotator calculations in which we retained only the spherically symmetric and dipole-dipole terms of the AD potential, which yields M = 3 (see Figures 1, 3, and 4). These calculations converge more rapidly with increasing N and usually yield even less rotationally inelastic scattering. For example Table 2 compares the converged inelastic transition probabilities

Table 2. Inelastic T → R transition probabilities for full (M = 9) and truncated (M = 3) AD potentials as functions of relative translational energy

E_{rel} (meV)	M = 9	M = 3
76	0.07	0.15
657	0.59	0.28
1550	0.90	0.82

$$P^R_{inel} = \sum_{j'_{sum} \neq 0} P^R_{j'_{sum}} \qquad (13)$$

for the two surfaces at three energies. In comparison to the RB potential, for which $P^R_{inel} \geq 0.97$ at all three energies, the total inelasticity is low at all energies studied for both surfaces in Table 2. Clearly the dipole-dipole term or even a small subset of low-order anisotropic terms do not account for most of the T-R energy transfer at J = 0.

The dramatic difference between the AD and the other potentials persists up to higher translational energies. For example, P^R_0 for the AD potential is 0.414 at 657 meV, and the sum of P^R_0, P^R_1, and P^R_2 is 0.713 (14), whereas, for example, for the BM potential these same quantities are 0.005 and 0.035, respectively, and the three largest values of $P^R_{j'_{sum}}$ occur for j'_{sum} = 12-14 (23).

A more detailed comparison of two of the surfaces at a higher energy, E_{rel} = 322 meV, is given in Table 3. This table compares $P^R_{j'_{sum}}$ for all energetically accessible values of j'_{sum} at this energy and also twelve selected value of $P^R_{j'_1 j'_2}$ (the transitions included are those for which $P^R_{j'_1 j'_2} > 0.035$ for the BM potential). We see that both $P^R_{j'_{sum}}$ distributions peak for j'_{sum} = 6-9 at this energy with a "shoulder" at j'_{sum} = 4-5. Individual transition probabilities typically, but not always, agree within a factor of two and for the most part the same individual final states have large transition probabilities for the two potentials. (Three other final states have larger probabilities for the RB potential — in particular, P^R_{22} = 0.055, P^R_{34} = 0.061, and P^R_{26} = 0.073.)

Table 3. Rigid-rotator transition probabilities for two potentials for E_{rel} = 322 meV

j'_{sum}	BM	RB	j'_1	j'_2	BM	RB
0	0.055	0.021	0	0	0.055	0.021
1	0.001	0.003	1	1	0.036	0.026
2	0.043	0.026	2	3	0.054	0.037
3	0.020	0.033	1	4	0.042	0.021
4	0.048	0.079	2	4	0.044	0.059
5	0.100	0.061	3	3	0.039	0.026
6	0.173	0.135	1	5	0.068	0.046
7	0.222	0.159	2	5	0.122	0.075
8	0.140	0.259	1	6	0.065	0.016
9	0.125	0.165	3	5	0.065	0.140
10	0.047	0.052	4	5	0.069	0.057
11	0.013	0.007	3	6	0.038	0.078
12	0.011	0.001				
13	0.002	0.000				
14	0.001	0.000				

Another perspective on the comparison of the BM and RB surfaces is provided in Figures 12 and 13. This figure shows quantum mechanical values (23,24) of $P^R_{j'_{sum}}$ for both potentials and quasiclassical trajectory values (24) of $P^R_{j'_{sum}}$ for the RB surface for two relative translational energies. The two sets of quantal results agree with each other much better than either agrees with the classical simulation. Thus, especially when we consider that the approaches used (19,21) to construct the two potentials were very different, we gain some confidence that the dynamically important features of the anisotropy of the potential are probably reasonably accurate for *both* analytical representations. We thus feel that it is very worthwhile to try to converge the V-V and V-V,R energy transfer probabilities for the RB potential or for the more convenient RBST modification of the RB potential.

Vibrating Rotator Calculations (13-16,22)

We consider the V-V,R process (1),

$$2HF(v=1,j=0) \rightarrow HF(v'_1=2,j'_1) + HF(v'_2=0,j'_2)$$

with total angular momentum J = 0. Therefore we again have $j_{12} = \ell = 0$, and we again sum over j'_{12} or ℓ' for a given j'_{sum} defined by

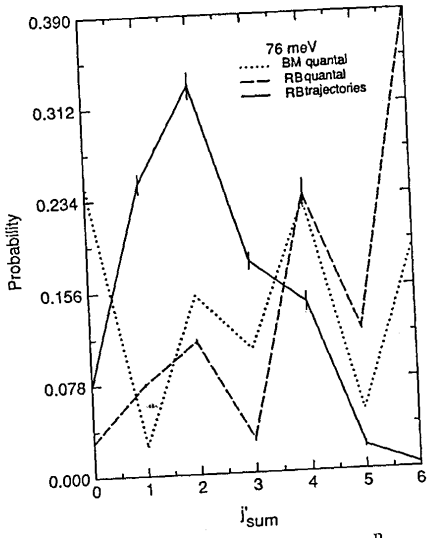

Figure 12. Rotational excitation probability $P^R_{j'_{sum}}$ as a function of j'_{sum} for E_{rel} =76 meV.

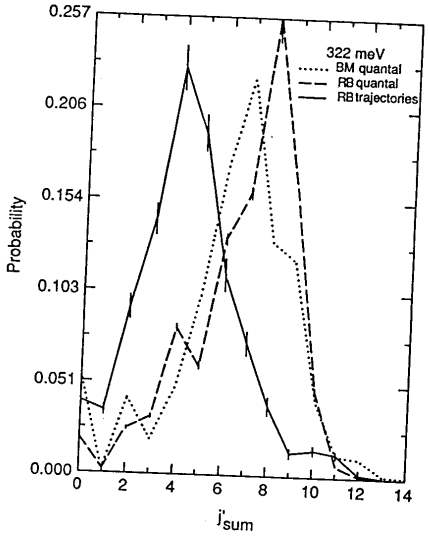

Figure 13. Same as Fig. 12 except for E_{rel} = 322 meV.

Equation (12); in this case the result is called $P^{VV}_{j'_{sum}}$. Summing $P^{VV}_{j'_{sum}}$ over j'_{sum} yields the total V-V,R transition probability, which is called P^{VV}. Selected results are given in Table 4, where the rows labelled 0-7 are $P^{VV}_{j'_{sum}}$, and the rows labelled "sum" are P^{VV}.

The largest N for which calculations were performed for the MAD potential is 948, and comparison (15) of these calculations to others with N = 694, 824, and 880 shows that the N = 948 calculations are well converged at E_{rel} = 2.455 meV and approximately converged at 76 meV. The largest N for which calculations have been performed on the RB potential is N = 694, which is not enough for quantitative convergence, but which is adequate for a discussion of trends. [For these calculations the V matrix was not calculated as accurately as for the calculations with the MAD and RBST potentials, and the sum of Equation (3) was truncated at M = 161, but these approximations should not matter

Table 4. V-V,R energy transfer probabilities

j'_{sum}	N = 694			N = 948	
	MAD	RB	RBST	MAD	RBST
	E_{rel} = 2.455 meV				
0	0.85	0.10	0.02	0.90	0.03
1	0.04	0.03	0.17	0.04	0.24
2	0.00	0.19	0.38	0.00	0.35
3[a]	0.00	0.20	0.42	0.00	0.37
sum	0.89	0.42	0.99	0.94	0.99
	E_{rel} = 76 meV				
0	0.81	0.00	0.00	0.73	0.00
1	0.05	0.01	0.05	0.03	0.05
2	0.06	0.01	0.02	0.09	0.02
3	0.01	0.01	0.05	0.01	0.05
4	0.00	0.02	0.06	0.00	0.06
5	0.00	0.02	0.06	0.00	0.06
6	0.00	0.02	0.09	0.00	0.09
7[a]	0.00	0.02	0.12	0.00	0.12
sum	0.93	0.12	0.45	0.87	0.45

[a]Highest value allowed by conservation of total energy at this E_{rel}.

for the present qualitative discussion.] To facilitate comparison of the results for the RB potential to those for the other potentials, the latter are tabulated for both N = 694 and N = 948. There are two major differences between the results for the RB and the MAD potential. The MAD potential predicts more V-V,R energy transfer, and it also predicts that the V-V,R process involves very little rotational excitation whereas the RB potential predicts a wide j'_{sum} distribution peaking for the higher energetically allowed values. We believe that the j'_{sum} distribution for the MAD potential is likely to be an artifact of the restricted rotational anisotropy of the AD potential.

Table 4 also shows that the RBST potential, despite the restriction to M = 23, predicts a broad j'_{sum} distribution similar to that obtained for the RB potential, but it predicts a higher value for the total V-V,R transition probability. It is not known at this time which potential is more accurate.

Further work is underway.

Conclusion

The use of supercomputers has allowed us to test the sensitivity of accurate quantal molecular energy transfer probabilities in diatom-diatom collisions to the choice of potential energy surface, even at total energies great enough to allow both diatoms to be vibrationally excited.

Acknowledgment

This work was supported in part by the National Science Foundation, the Minnesota Supercomputer Institute, and the Control Data Corporation.

Literature Cited

1. Kondratiev, V. N.: Nikitin, E. E. Gas Phase Reactions; Springer-Verlag; Berlin, 1981.
2. Yardley, J. T. Introduction to Molecular Energy Transfer; Academic Press: New York, 1980.
3. Secrest, D. In Atom-Molecule Collision Theory; Bernstein, R. B., Ed., Plenum: New York, 1979; p. 377.
4. Slater, J. C. Quantum Theory of Molecules and Solids, Vol. 1; McGraw-Hill, New York, 1963, Appendix 2.
5. Arthurs, A. M.; Dalgarno, A. Proc. Roy. Soc. Lond. Ser. A 1960, 256, 540.
6. Davison, W. D. Discussions Faraday Soc. 1962, 33, 71.
7. Green, S. J. Chem. Phys. 1975, 62, 2271.
8. Bellman, R.; Kalaba, R. Proc. Natl. Acad. Sci. 1956, 42, 629.
9. Bellman, R.; Kalaba, R.; Wing, G. M. J. Math. Phys. 1960, 1, 280.
10. Bellman, R.; Kalaba, R.; Wing, G. M. Proc. Natl. Acad. Sci. 1960, 46, 1646.
11. Light, J. C.; Walker, R. B. J. Chem. Phys. 1976, 65, 4272.

12. Truhlar, D. G.; Harvey, N. M.; Onda, K.; Brandt, M. A. In: Algorithms and Computer Codes for Atomic and Molecular Quantum Scattering Theory, Vol. 1; Lawrence Berkeley Laboratory: Berkeley, 1979, p. 220.
13. Schwenke, D. W.; Truhlar, D. G. Theor. Chim. Acta 1986, 69, 175.
14. Schwenke, D. W.; Truhlar, D. G. In: Supercomputer Simulations in Chemistry, Dupuis, M., Ed. Springer-Verlag: Berlin, 1986, p. 165.
15. Schwenke, D. W.; Truhlar, D. G. Theor. Chim. Acta, in press.
16. Schwenke, D. W.; Truhlar, D. G. unpublished.
17. Alexander, M. H; DePristo, A. E. J. Chem. Phys. 1976, 65, 5009.
18. Poulsen, L. L.; Billing, G. D.; Steinfeld, J. I. J. Chem. Phys. 1978, 68, 5121.
19. Brobjer, J. T.; Murrell, J. N. Mol. Phys. 1983, 50, 885.
20. Cournoyer, M. E.; Jorgensen, W. L. Mol. Phys. 1984, 51, 119.
21. Redmon, M. J.; Binkley, J. S., J. Chem. Phys., in press.
22. Schwenke, D. W.; Truhlar, D. G. In: Supercomputer Applications. Numrich, R. W., Ed. Plenum: New York, 1985, p. 295.
23. Schwenke, D. W.; Truhlar, D. G. J. Comp. Chem., in press.
24. Schwenke, D. W.; Truhlar, D. G.; Coltrin, M. E. J. Chem. Phys., in press.
25. Poulsen, L. L.; Billing, G. D. Chem. Phys. 1979, 36, 271.
26. Poulsen, L. L.; Billing, G. D. Chem. Phys. 1980, 46, 287.
27. Poulsen, L. L.; Billing, G. D. Chem. Phys. 1980, 53, 389.
28. Coltrin, M. E.; Marcus, R. A. J. Chem. Phys. 1980, 73, 2179.
29. Coltrin, M. E.; Koszykowski, M. L.; Marcus, R. A. J. Chem. Phys. 1980, 73, 3643.
30. Coltrin, M. E.; Marcus, R. A. J. Chem. Phys. 1980, 73, 4390.
31. Coltrin, M. E.; Marcus, R. A. J. Chem. Phys. 1982, 76, 2379.
32. Sileo, R. N.; Cool, T. A. J. Chem. Phys. 1976, 65, 117.
33. Maillard, D.; Silvi, B. Mol. Phys. 1980, 40, 933.
34. Kollman, P. A. In Chemical Applications of Atomic and Molecular Electrostatic Potentials; Truhlar, D. G., Ed. Plenum Press: New York, 1981, p. 243.
35. Gianturco, F. A.; Lamanna, U. T.; Battiglia, F. Int. J. Quantum Chem. 1981, 19, 217.
36. Truhlar, D. G.; Brown, F. B; Schwenke, D. W.; Steckler, R.; Garrett, B. C. In Comparison of Ab Initio Quantum Chemistry with Experiment for Small Molecules, Bartlett, R. B., Ed. Reidel: Dordrecht, Holland, 1985, p. 95.
37. Hancock, G. C.; Rejto, P.; Steckler, R.; Brown, F. B.; Schwenke, D. W.; and Truhlar, D. G. J. Chem. Phys. 1985, 85, 4997.
38. Hancock, G. C.; Truhlar, D. G.; Dykstra, C. E., to be published.
39. Schwenke, D. W.; Truhlar, D. G. Computer Phys. Commun. 1984, 34, 57.
40. Alexander, M. H.; DePristo, A. E. J. Chem. Phys. 1977, 66, 2166.
41. Alexander, M. H. J. Chem. Phys. 1980, 73, 5135.

RECEIVED June 15, 1987